

Original Research Paper

# High Density Salt and Pepper Noise Filter based on Shepard Interpolation Method

<sup>1</sup>Chaipichit Cumpim and <sup>2</sup>Rachu Punchalard

<sup>1</sup>The Electrical Engineering Graduate Program,

<sup>2</sup>Department of Telecommunication Engineering,

Faculty of Engineering, Mahanakorn University of Technology, Bangkok, Thailand

## Article history

Received: 05-05-2017

Revised: 19-06-2017

Accepted: 19-07-2017

Corresponding Author:

Chaipichit Cumpim

The Electrical Engineering  
Graduate Program, Faculty of  
Engineering, Mahanakorn  
University of Technology,  
Bangkok, Thailand  
Email: chaipichit@gmail.com

**Abstract:** This paper has proposed the technique in order to remove salt-and-pepper noise from the corrupted image. The proposed scheme consists of two steps. The first, the adaptive median filter is applied to noisy image for detecting noisy and noise-free pixels. Finally, the output image of previous step will be divided into many non-overlapping windows of which the noise-free pixel values are used to compute the new pixel value by the Shepard method. The experiment results of our approach had shown the better performance than the existing method.

**Keywords:** Denoise, Filter, Impulse Noise, Salt-and-Pepper Noise, Shepard Interpolation Method

## Introduction

The output images of the transmission system and camera sensor are always contaminated with the impulse noises. The impulse noises have two common types which are Salt-and-Pepper (SPN) noise and random valued noise (Bovik, 2005). In this research, we have focused on the SPN. The SPN model of the corrupted image  $y$  which is defined as follow:

$$y(i, j) = \begin{cases} s_{\min} & \text{with probability } p \\ s_{\max} & \text{with probability } q \\ x(i, j) & \text{with probability } 1 - p - q \end{cases} \quad (1)$$

where,  $p + q$  denote the total probability of occurrence of SPN,  $x$  denote the original image,  $[s_{\min}, s_{\max}]$  denote the dynamic range of the pixel values of the image  $x(s_{\min} \leq x(i, j) \leq s_{\max})$  and  $(i, j)$  denote the pixel location. In this study, the original and corrupted image with size  $M \times N$  is the gray image. The pixel location  $(i, j)$  can be defined as  $(i, j) \in A \equiv \{1, \dots, M\} \times \{1, \dots, N\}$ . There are many methods have tried to restore the corrupted images with SPN. Each method will be introduced as follows.

For the SPN filtering techniques, they can be classified into two categories which are the median-based and non-median-based filtering. The first category is the median filter (MF) (Bovik, 2005). It is widely used for the SPN filtering. It is a faster and non-complexity

method which is the best performance for the low-level noise density of SPN. The other is the Adaptive Median Filter (AMF) (Gonzalez and Woods, 2006), this method has improved the MF by increasing the window size of sliding window for the median value finding. The next approach is the Center Weight Median filter (CWM) which has proposed by (Ko and Lee, 1991). It has applied the weight adjustment to the center pixel value of each sliding window before the median filter has employed. The next method is the Progressive Switching median filter (PSW) (Wang and Zhang, 1999). It contains two phases that are the noise detection and restoration phases. The two steps have repeated operation to noisy image. The other method is the Adaptive Center Weight Median filter (ACWM) (Chen and Wu, 2001). It has used the different of the resulting image of CWM and the corrupted image to detect the noisy pixel before the median value is replaced on the noise candidate pixel. The next method is the Decision-Based Algorithm (DBA) (Srinivasan and Ebenezer, 2007), this method uses the maximal and minimal values of the dynamic range in order to identify the noisy pixels. In the next phase, the median value of window or the neighboring value will replace the noisy pixel. For the method in (Toh and Isa, 2010), it is the Noise Adaptive Fuzzy Switching Median filter (NASFM) which applies the fuzzy rule to the histogram of the corrupted image for noise detecting. Next step, the median value of sub-window will replace on the noisy

pixel. The other method is the Modified Decision Based Unsymmetric Trimmed Median Filter (MDBUTMF) (Esakkirajan *et al.*, 2011), it has proposed the restoring of the corrupted pixel with the trimmed median value. The next method is the Fast Switch Based Median-Mean Filter (FSBMMF) (Vijaykumar *et al.*, 2014), this method uses the maximum and minimum pixel values to classify the corrupted pixel. In the next stage, the median or mean value based on the number of the uncorrupted pixels of sub-window will replace the noisy pixel. The last method is the Continued Fractions Interpolation Filter (CFIF) (Bai *et al.*, 2014), this technique is classified as the non-median-base filter group. It applies the continued fractions interpolation method in order to calculate the new pixel value of the corrupted pixel after the noise detection step. It uses the same noise detection method as FSBMMF.

In this study, we will show the technique to remove the SPN. Our method consists of two steps. The first step, we use the AMF to detect the SPN on the corrupted image as presented in (Nikolova *et al.*, 2008). Finally, the new pixel value which calculate by using the noise-free pixels of the divided window to restore the noisy pixel. In the calculating method, it use the Shepard interpolation method (Shepard, 1968).

### Brief Description of Shepard Interpolation Method

In this study, we have used the Shepard interpolation method (Shep) in order to interpolate the new pixel value of the corrupted pixel. This approach is the simple method for the scatter data interpolation. It usually uses on the surface interpolating in the geography system or computer graphic. For Several improved Shep methods, they have proposed by many authors as shown in (Barnhill, 1977; Gordon and Wixom, 1978; Pmathrmacutal *et al.*, 2009). In this section, we use Fig. 1 to describe the Shep method. The form of this method is defined as shown in (2). From Fig. 1, the known value points which represent by  $y(i_k, j_k)$  ( $k = 1, \dots, K$ ) are black squares and the unknown value point which represent by  $z(i_0, j_0)$  is the white square. For the known points, they are used to interpolate value of the unknown point as shown in the following form:

$$z(i_0, j_0) = \frac{\sum_{k=1}^K w_k(i_0, j_0) y(i_k, j_k)}{\sum_{k=1}^K w_k(i_0, j_0)} \quad (2)$$

where,  $w_k(i_0, j_0) = \frac{1}{(d_k)^2}$  is the weight function and  $d_k = \sqrt{(i_0 - i_k)^2 + (j_0 - j_k)^2}$  is the Euclidian distance between  $(i_0, j_0)$  and  $(i_k, j_k)$ .

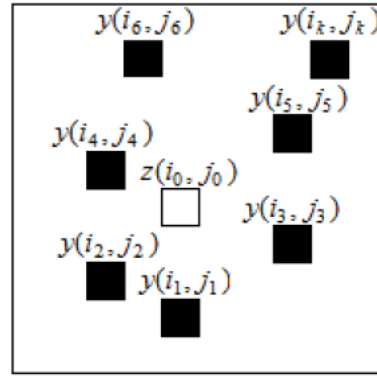


Fig. 1. The scatter data

### Proposed Method

For our method, it contains two steps. The first step presents the noise detecting and the last step shows that the Shep method is used for removing SPN. The detail of each step will describe as follows.

#### Salt-and-Pepper Noise Identification

##### Algorithm 1 AMF

For each pixel  $(i, j) \in A$  of contaminated image  $y$  and restored image  $Y_f$ , do

- 1) Initialize  $w = 1, h = 1, w_{\max} = 39$ .
- 2) Compute  $S_{\min_w}, S_{\max_w}$  and  $S_{\text{med}_w}$ .
- 3) If  $S_{\min_w} < S_{\text{med}_w} < S_{\max_w}$ , go to step 5);  
 Otherwise,  $w = w + h$
- 4) If  $w \leq w_{\max}$ , go to step 2);  
 Otherwise  $Y_f(i, j) = S_{\text{med}_{w_{\max}}}$  and stop.
- 5) If  $S_{\min_w} < y(i, j) < S_{\max_w}$ ,  $(i, j)$  is uncorrupted,  
 $Y_f(i, j) = y(i, j)$ ; Otherwise  $Y_f(i, j) = S_{\text{med}_w}$  and stop.

For this step, we must search the noise-free and noisy pixels on the corrupted image to generate noisy and noise-free pixel sets, vertical and horizontal pixel location arrays and mask image. The noise-free pixel positions, which will obtain from this step, are used to calculate the new pixel value for replacing the noisy pixel by the Shep method. We use the AMF to detect the SPN on the corrupted image as described in (Nikolova *et al.*, 2008). The AMF algorithm is shown in Algorithm 1. We define symbols  $S_{\min_w}, S_{\max_w}, S_{\text{med}_w}$ , to denote minimum, maximum and median values of sub-window  $S$  with size  $w$ , respectively.

The noisy pixel set  $N_f$  can detect by comparing the restored image  $Y_f$  of AMF with the corrupted image  $y$  with size  $M \times N$ . This detecting will generate the corrupted pixel set as:

$$N_n = \{(i, j) \in A : Y_f(i, j) \neq y(i, j)\} \quad (3)$$

where,  $(i, j)$  is the noisy pixel location. For the noise-free pixel set  $N_f$ , it defines as:

$$N_f = \{(i, j) \in A : Y_f(i, j) = y(i, j)\} \quad (4)$$

where,  $N_f = A \setminus N_n$ . In this step, the noise density  $N_d$  is calculated as:

$$N_d = \frac{N_c}{MN} \times 100 \quad (5)$$

where,  $N_c$  is the number of the member in the set  $N_n$ . This parameter is used to define the non-overlapping window size  $w_d$  as show in Table 1. These non-overlapping window size  $w_d$  values have obtained from process of trial and error. This process will be shown in section 4.2.

After the noisy and noise-free pixels sets were created, we have made the mask image  $M_n$  with size  $M \times N$  by using the condition of Noisy and noise-free pixel sets. The mask image form is given by:

$$M_n(i, j) = \begin{cases} 1 & (i, j) \in A : Y_f(i, j) = y(i, j) \\ 0 & (i, j) \in A : Y_f(i, j) \neq y(i, j) \end{cases} \quad (6)$$

If  $M_n(i, j)$  equals one, this location is the noisy pixel, while the noise-free pixels represent  $M_n(i, j) = 0$ .

For the vertical  $L_v$  and horizontal  $L_h$  pixel location arrays with size  $M \times N$ , they will be created by (7) and (8). The form of  $L_v$  is defined as:

$$L_v(i, j) = i; (i, j) \in A \quad (7)$$

and The form of  $L_h$  is given by:

$$L_h(i, j) = j; (i, j) \in A \quad (8)$$

### Noise Restoration

In this section, the restored image  $Y_f$ , mask image  $M_n$ , vertical  $L_v$  and horizontal  $L_h$  pixel location arrays was divided into non-overlapping windows as shown in Fig. 2 which similar to (Chang *et al.*, 2007; Cumpim *et al.*, 2016) before the restoring noisy pixels process is started. We define  $S_{Y_f}$ ,  $S_{M_n}$ ,  $S_{L_v}$  and  $S_{L_h}$  as non-overlapping window of the restored image, mask image, vertical and horizontal pixel location, respectively. The non-overlapping window size is defined as  $w_v \times w_h$  where  $w_h = w_v = w_d$ . We can define the non-overlapping window  $w_d$  as shown in Table 1.

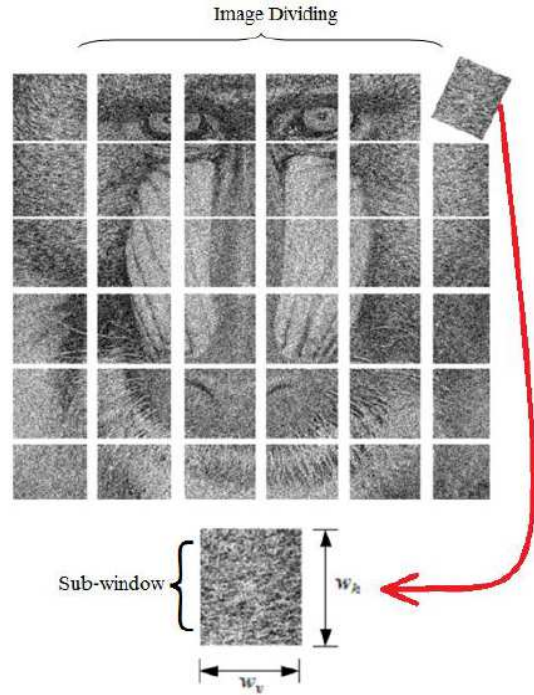


Fig. 2. Dividing image as sub-windows

Table 1. Window size of sub-window

Noise density ( $N_d\%$ )	Window size ( $w_d$ )
$N_d \leq 20$	3
$20 < N_d \leq 50$	4
$50 < N_d \leq 70$	7
$70 < N_d \leq 80$	8
$N_d > 80$	12

After the dividing process has finished, the restored noisy pixels is begun by using Shep method. In each non-overlapping window of  $S_{Y_f}$ ,  $S_{M_n}$ ,  $S_{L_v}$  and  $S_{L_h}$ , they must locate as the same position. We use (2) to calculate the new pixel value of each noisy pixel in  $S_{Y_f}$ . The noisy and noise-free pixel can be checked by the value of  $S_{M_n}$ . We define the new pixel value as  $z(i_0, j_0)$  in (2) and define all of noise-free pixel values of  $S_{Y_f}$  as  $y(i_k, j_k)$  ( $k = 1, \dots, K$ ) where  $K$  is the number of noise-free pixels of  $S_{Y_f}$ . For the location of noisy pixel  $(i_0, j_0)$ , it obtain from  $S_{L_v}$  and  $S_{L_h}$  by checking the location on  $S_{M_n}$ . Besides, the location of noise-free pixels  $(i_k, j_k)$ ; ( $k = 1, \dots, K$ ) can obtain from  $S_{L_v}$  and  $S_{L_h}$  too. After we define variables in (2), the noisy pixel value in each non-overlapping window can be calculated by (2).

### Experiment and Results

We implement our method to comparing with the conventional methods: (MF) (Bovik, 2005), (AMF) (Gonzalez and Woods, 2006), FSBMMF (Vijaykumar *et al.*, 2014), CFIF (Bai *et al.*, 2014) and (Chang *et al.*, 2007; Cumpim *et al.*, 2016). The MATLAB

software is applied in order to implement every method. We use four grey images with size 512×512, which are Baboon, Barbara, Boat and Lena images as shown in Fig. 3. They are tested by our method and conventional methods. These images are added the SPN with the noise density from 10 to 90% as shown in Fig. 4.

For the evaluating of this experiment, we have used the Peak Signal-to-Noise Ratio (PSNR) (Bovik, 2005), Mean of Structural Similarity Index (MSSIM) (Wang *et al.*, 2004), Signal-to-Noise Ratio in spatial domain (SNR) (Gonzalez and Woods, 2006) and visual quality of the resulting images. For *PSNR*, it is given by:

$$PSNR = 10 \log \frac{255^2}{\frac{1}{MN} \sum_{i=1}^M \sum_{j=1}^N (x(i,j) - z(i,j))^2} \quad (9)$$

where,  $x$  and  $z$  denote an original and filtering images and  $M \times N$  is a size of both images. For *MSSIM*, it can be defined as follow:

$$MSSIM = \frac{1}{MN} \sum_{i=1}^M \sum_{j=1}^N SSIM(i,j) \quad (10)$$

where, *SSIM* is expressed by:

$$SSIM = \frac{(2\mu_x\mu_z + C_1)(2\sigma_{xz} + C_2)}{((\mu_x)^2 + (\mu_z)^2 + C_1)((\sigma_x)^2 + (\sigma_z)^2 + C_2)} \quad (11)$$

where, *SSIM* denotes the structural similarity index,  $\mu_x$  and  $\mu_z$  denote the mean of the original and restored images,  $\sigma_x$  and  $\sigma_z$  denotes the standard deviation of the original and restored images,  $\sigma_{xz}$  denotes the covariance of  $x$  and  $z$  and the constants are represented by  $C_1$  and  $C_2$ . resulting images. For *SNR*, it is given by:

$$SNR = 10 \log \frac{\sum_{i=1}^M \sum_{j=1}^N (x(i,j))^2}{\sum_{i=1}^M \sum_{j=1}^N (x(i,j) - z(i,j))^2} \quad (12)$$

and can be defined as follow *MSSIM*

### Noise Removal Performance

For Table 2 and, it shows that the proposed method is higher than the other methods. Although the proposed method is lower *PSNR* than the existing methods between 10 and 40% noise density level, the proposed method is higher *PSNR* than the conventional method between 50 and 90% noise density level.

For Table 3, our method is higher *MSSIM* than the other methods. For 10 and 30% noise density level, the proposed method is lower *MSSIM* than the existing methods, while the proposed method is higher *MSSIM* than the conventional methods between 40 and 90% noise density level.

Table 2. *PSNR* of different methods

Images	Methods	Noise density (%)								
		10	20	30	40	50	60	70	80	90
Baboon	AMF	28.30	27.18	25.88	24.69	23.52	22.39	21.31	20.17	18.70
FSBMMF		<b>32.84</b>	29.40	27.20	25.53	24.01	22.73	21.43	20.24	18.64
CFIF		32.32	28.92	26.73	25.12	23.85	22.73	21.74	20.82	19.63
(Cumpim <i>et al.</i> 2016)		32.82	29.66	27.68	26.57	25.35	24.44	23.46	22.56	21.11
Proposed		32.82	<b>29.66</b>	<b>27.87</b>	<b>26.57</b>	<b>25.35</b>	<b>24.44</b>	<b>23.46</b>	<b>22.56</b>	<b>21.38</b>
Barbara	AMF	28.81	27.69	26.42	25.21	24.07	23.03	21.95	20.70	19.11
FSBMMF		33.17	29.83	27.71	26.04	24.62	23.28	21.92	20.17	17.94
CFIF		31.96	28.77	26.86	25.47	24.28	23.28	22.32	21.07	19.05
(Cumpim <i>et al.</i> 2016)		33.40	30.28	28.36	27.20	26.02	25.05	24.10	23.07	21.58
Proposed		<b>33.40</b>	<b>30.28</b>	<b>28.62</b>	<b>27.20</b>	<b>26.02</b>	<b>25.05</b>	<b>24.10</b>	<b>23.07</b>	<b>21.93</b>
Boat	AMF	23.04	23.00	22.91	22.86	22.67	22.33	21.55	18.11	10.83
FSBMMF		33.96	32.14	30.18	28.56	27.25	25.68	24.28	22.65	20.23
CFIF		<b>37.92</b>	34.03	31.35	29.18	27.58	25.54	23.58	21.50	18.67
(Cumpim <i>et al.</i> 2016)		37.84	34.32	31.66	29.50	27.74	25.99	24.24	22.59	20.19
Proposed		37.84	<b>34.32</b>	<b>31.66</b>	<b>29.87</b>	<b>28.81</b>	<b>27.46</b>	<b>26.27</b>	<b>25.23</b>	<b>23.07</b>
Lena	AMF	39.15	36.89	34.99	32.98	31.31	29.84	28.02	26.03	23.21
FSBMMF		42.84	38.58	35.93	33.47	31.10	29.20	26.96	24.50	21.58
CFIF		<b>42.90</b>	<b>38.68</b>	<b>36.28</b>	<b>33.89</b>	32.00	30.25	28.16	25.91	22.62
(Cumpim <i>et al.</i> 2016)		40.66	37.42	35.07	33.68	32.40	31.16	30.00	28.52	25.69
Proposed		40.66	37.42	35.29	33.76	<b>32.49</b>	<b>31.16</b>	<b>30.00</b>	<b>28.58</b>	<b>26.70</b>

Table 3. *MSSIM* of different methods

Images	Methods	Noise density (%)								
		10	20	30	40	50	60	70	80	90
Baboon	AMF	0.344	0.344	0.342	0.340	0.337	0.333	0.320	0.252	0.066
FSBMMF		0.897	0.876	0.841	0.795	0.737	0.668	0.585	0.481	0.347
CFIF		<b>0.969</b>	0.931	0.884	0.830	0.759	0.682	0.586	0.478	0.344
(Cumpim <i>et al.</i> 2016)		0.964	0.922	0.871	0.812	0.741	0.663	0.570	0.459	0.308
Proposed		0.968	<b>0.932</b>	<b>0.892</b>	<b>0.851</b>	<b>0.800</b>	<b>0.744</b>	<b>0.676</b>	<b>0.593</b>	<b>0.469</b>
Barbara	AMF	0.606	0.604	0.600	0.593	0.584	0.573	0.544	0.424	0.110
FSBMMF		0.933	0.917	0.891	0.856	0.814	0.763	0.698	0.611	0.488
CFIF		<b>0.978</b>	<b>0.952</b>	0.919	0.878	0.829	0.768	0.691	0.589	0.444
(Cumpim <i>et al.</i> 2016)		0.973	0.943	0.908	0.867	0.818	0.760	0.687	0.571	0.365
Proposed		0.977	0.951	<b>0.922</b>	<b>0.891</b>	<b>0.855</b>	<b>0.811</b>	<b>0.763</b>	<b>0.697</b>	<b>0.605</b>
Boat	AMF	0.934	0.922	0.899	0.867	0.827	0.775	0.712	0.626	0.497
FSBMMF		<b>0.981</b>	<b>0.957</b>	0.927	0.890	0.843	0.780	0.699	0.593	0.457
CFIF		0.979	0.956	0.926	0.889	0.842	0.783	0.703	0.600	0.427
(Cumpim <i>et al.</i> 2016)		0.978	0.954	0.927	0.899	0.868	0.826	0.782	0.729	0.636
Proposed		0.978	0.954	<b>0.929</b>	<b>0.899</b>	<b>0.868</b>	<b>0.826</b>	<b>0.782</b>	<b>0.730</b>	<b>0.640</b>
Lena	AMF	0.796	0.794	0.790	0.785	0.779	0.767	0.738	0.570	0.115
FSBMMF		0.969	0.961	0.949	0.930	0.906	0.875	0.832	0.771	0.663
CFIF		<b>0.991</b>	<b>0.978</b>	<b>0.962</b>	0.940	0.912	0.874	0.819	0.747	0.631
(Cumpim <i>et al.</i> 2016)		0.990	0.977	0.961	0.940	0.912	0.877	0.821	0.734	0.525
Proposed		0.990	0.977	0.961	<b>0.942</b>	<b>0.923</b>	<b>0.900</b>	<b>0.874</b>	<b>0.838</b>	<b>0.776</b>

Table 4. *SNR* of different methods

Images	Methods	Noise density (%)								
		10	20	30	40	50	60	70	80	90
Baboon	AMF	22.61	21.48	20.19	19.00	17.83	16.70	15.62	14.48	13.01
FSBMMF		<b>27.14</b>	23.71	21.51	19.84	18.32	17.04	15.74	14.55	12.95
CFIF		26.63	23.22	21.03	19.43	18.16	17.04	16.05	15.12	13.94
(Cumpim <i>et al.</i> 2016)		27.13	23.97	21.99	20.88	19.66	18.75	17.77	16.86	15.42
Proposed		27.13	<b>23.97</b>	<b>22.18</b>	<b>20.88</b>	<b>19.66</b>	<b>18.75</b>	<b>17.77</b>	<b>16.86</b>	<b>15.69</b>
Barbara	AMF	22.92	21.80	20.53	19.32	18.19	17.15	16.06	14.81	13.23
FSBMMF		27.28	23.94	21.82	20.15	18.73	17.39	16.03	14.28	12.06
CFIF		26.07	22.88	20.98	19.58	18.39	17.39	16.43	15.18	13.16
(Cumpim <i>et al.</i> 2016)		27.52	24.40	22.47	21.32	20.13	19.16	18.21	17.18	15.70
Proposed		<b>27.52</b>	<b>24.40</b>	<b>22.74</b>	<b>21.32</b>	<b>20.13</b>	<b>19.16</b>	<b>18.21</b>	<b>17.18</b>	<b>16.04</b>
Boat	AMF	23.04	23.00	22.91	22.86	22.67	22.33	21.55	18.11	10.83
FSBMMF		<b>33.96</b>	32.14	30.18	28.56	27.25	25.68	24.28	22.65	20.23
CFIF		37.92	34.03	31.35	29.18	27.58	25.54	23.58	21.50	18.67
(Cumpim <i>et al.</i> 2016)		37.84	34.32	31.66	29.50	27.74	25.99	24.24	22.59	20.19
Proposed		37.84	<b>34.32</b>	<b>31.66</b>	<b>29.87</b>	<b>28.81</b>	<b>27.46</b>	<b>26.27</b>	<b>25.23</b>	<b>23.07</b>
Lena	AMF	33.99	31.72	29.82	27.81	26.14	24.67	22.85	20.87	18.05
FSBMMF		37.67	33.41	30.77	28.30	25.93	24.03	21.79	19.34	16.41
CFIF		<b>37.73</b>	<b>33.51</b>	<b>31.11</b>	<b>28.73</b>	26.83	25.08	22.99	20.74	17.45
(Cumpim <i>et al.</i> 2016)		35.49	32.25	29.90	28.51	27.23	25.99	24.84	23.36	20.52
Proposed		35.49	32.25	30.12	28.59	<b>27.32</b>	<b>25.99</b>	<b>24.84</b>	<b>23.41</b>	<b>21.54</b>

For Table 4, our approach is higher *SNR* than the other methods. For 10 and 40% noise density level, the proposed technique is lower *SNR* than the existing methods, while the proposed method is higher *SNR* than the conventional methods between 40 and 90 % noise density level.

For Fig. 5b, is show that the region of interest (ROI) of original Barbara image as shown in Fig. 5a. Figure 5c show ROI of Barbara image with 60% noise density.

Even if AMF, FSBMMF and CFIF can remove SPN as shown in Fig. 6d-6f, respectively, these ROI are not smooth. For Fig. 6g and 6h, they are ROI of (Chang *et al.*, 2007; Cumpim *et al.*, 2016) and our method which are smooth image.

For Fig. 6, the show the original and results image of full Barbara image. Figure 6a shows the image with 60% noise density level. Figure 6b-6f shows the results image of AMF, FSBMMF, CFIF, (Chang *et al.*, 2007;

Cumpim *et al.*, 2016) and proposed methods, respectively. The result of our method is smoother than

the conventional methods and is better edge preserving than the other methods.

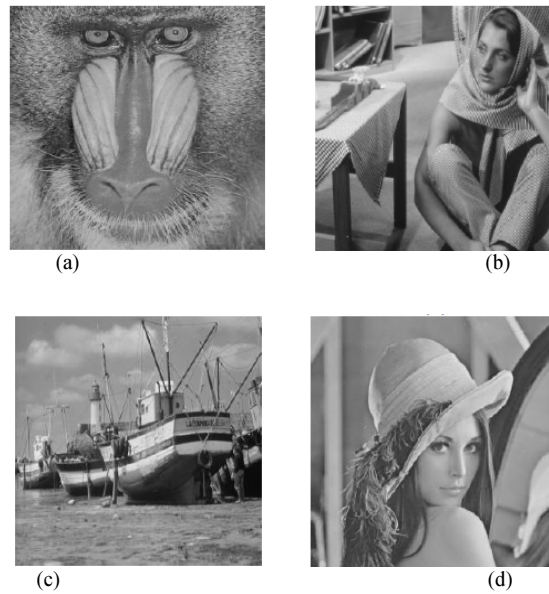


Fig. 3. Original images: (a) Baboon, (b) Barbara, (c) Boat and (d) Lena

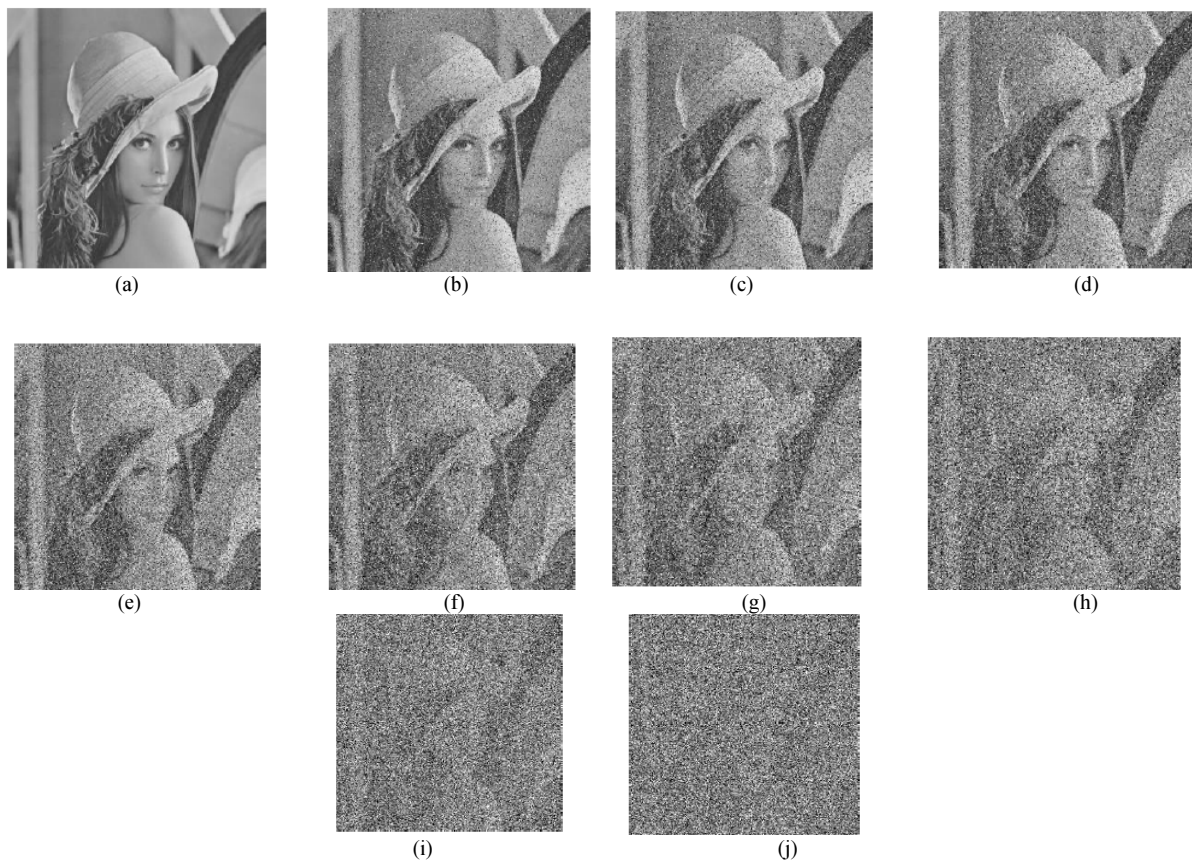


Fig. 4. Lena image with SPN (a) Original, (b-j) the corrupted Lena image with 10-90% SPN

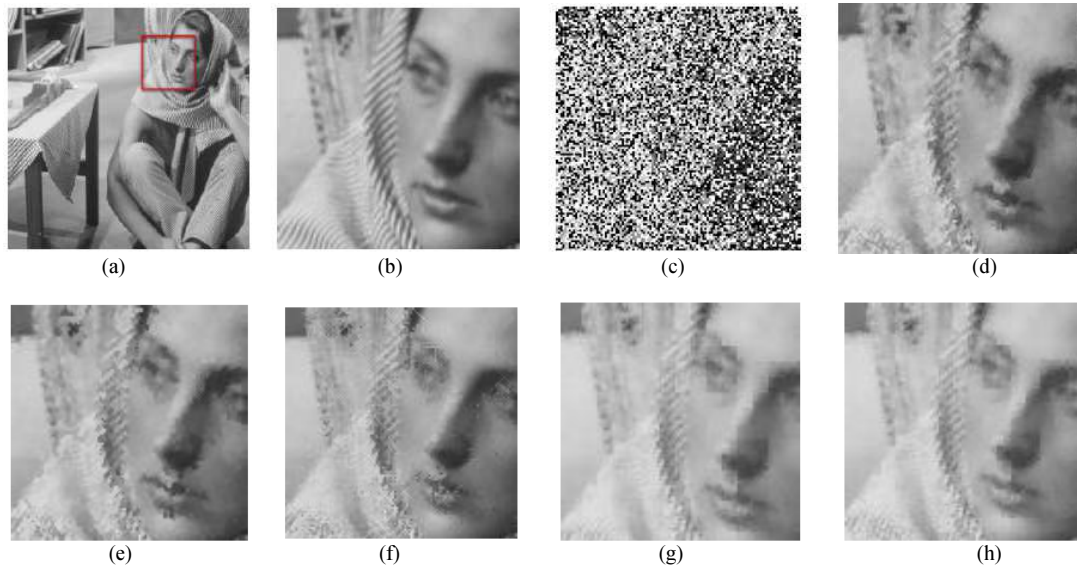


Fig. 5. (a) Original Barbara image (b) ROI of original Barbara image (c) ROI of the corrupted Barbara image with 60% SPN. The ROI resulting image (d) AMF, (e) FSBMMF, (f) CFIF, (g) (Chang *et al.*, 2007; Cumpim *et al.*, 2016) and (h) Proposed

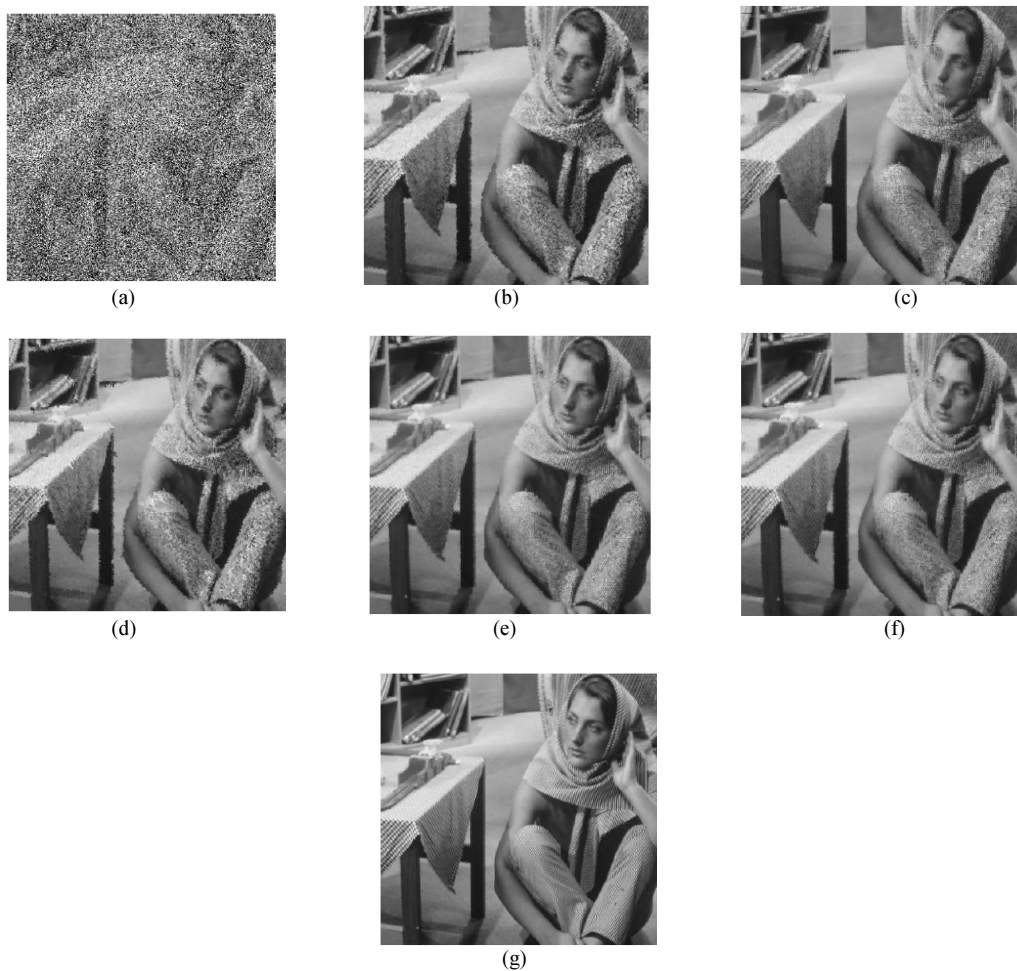


Fig. 6. The result of the experiment for Barbara image (a) the corrupted Barbara image with 60% SPN. Restoration results (b) AMF, (c) FSBMMF, (d) CFIF, (e) (Chang *et al.*, 2007; Cumpim *et al.*, 2006), (f) proposed and (g) original image

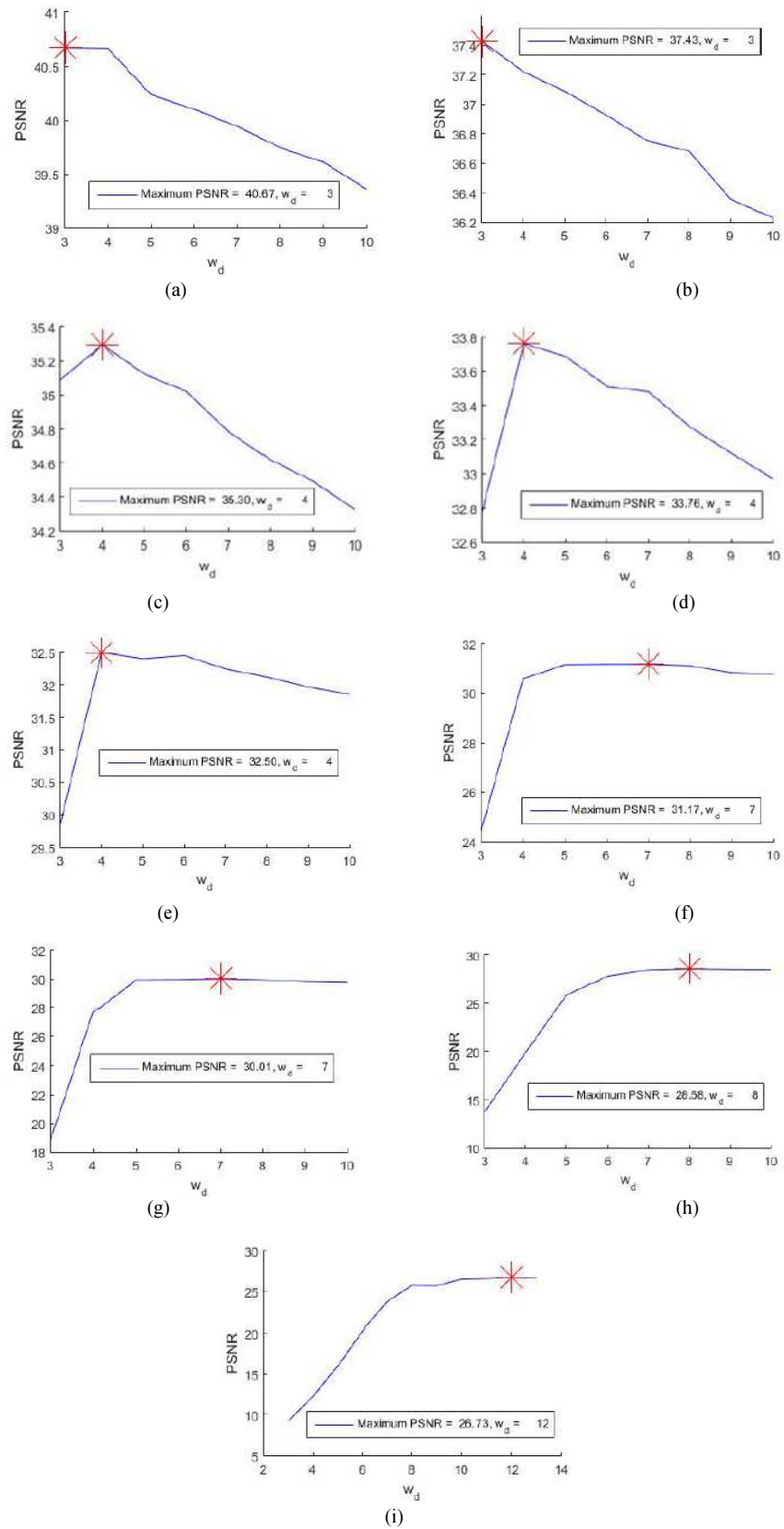


Fig. 7. Effect of non-overlapping window size ( $w_d$ ); (a) 10%; (b) 20%; (c) 30%; (d) 40%; (e) 50%; (f) 60%; (g) 70% (h) 80% (i) 90%

### Selection of Non-Overlapping Window Size ( $w_d$ )

The proposed method is required non-overlapping window size ( $w_d$ ). The selection of  $w_d$  is similar to (Toygar *et al.*, 2013). We have tested the Lena image with 10-90% noise density by varying the  $w_d$  {3, 4, 5, ..., 11, 12, 13} as shown in Fig. 7. Considering Fig. 7a-7i, we choose the best parameters of  $w_d$  from the maximum PSNR value which is shown by the red marker. This parameter has shown in Table. 1. The window size ( $w_d$ ) is decreasing value at low noise density while it is increasing value at high noise density.

### Conclusion

Our method which presented in this study was applied by using the Shepard interpolation method for replacing the noisy pixels. The detection of the noisy pixels has used the adaptive filter before each non-overlapping window will use the Shepard method to interpolate the new pixel value of each noisy pixel. In our method, the noise-free pixels are unchanged. The performance of proposed method, which uses the peak-signal-to-noise ratio, the mean of structural similarity index and visual quality, has better than the conventional method.

### Author's Contributions

All authors equally contributed in this work.

### Ethics

This article is original and contains unpublished material. The corresponding author confirms that all of the other authors have read and approved the manuscript and no ethical issues involved.

### References

Bai, T., J. Tan, M. Hu and Y. Wang, 2014. A novel algorithm for removal of salt and pepper noise using continued fractions interpolation. *Signal Process.*, 102: 247-255. DOI: 10.1016/j.sigpro.2014.03.023

Barnhill, R.E., 1977. *Mathematical Software*, Elsevier.

Bovik, A.C., 2005. *Handbook of Image and Video Processing (Communications, Networking and Multimedia)*. 1st Edn., Academic Press, Inc., USA.

Chang, C.C., C.C. Lin and Y.S. Hu, 2007. An SVD oriented watermark embedding scheme with high qualities for the restored images. *Int. J. Innovative Comput. Inform. Control*, 3: 609-620.

Chen, T. and H.R. Wu, 2001. Adaptive impulse detection using center-weighted median filters. *IEEE Signal Process. Lett.*, 8: 1-3. DOI: 10.1109/97.889633

Cumpim, C., R. Punalard, K. Janchitrapongvej and C. Kimpan, 2016. Salt-and-pepper noise removing by Shepard interpolation method. *Proceedings of the 13th International Conference on Electrical Engineering/Electronics, Computer, Telecommunications and Information Technology*, Jun. 28-Jul. 1, IEEE Xplore Press, Chiang Mai, Thailand, pp: 1-5. DOI: 10.1109/ECTICon.2016.7561486

Esakkirajan, S., T. Veerakumar, A.N. Subramanyam and C.H. PremChand, 2011. Removal of High Density Salt and Pepper Noise Through Modified Decision Based Unsymmetric Trimmed Median Filter. *IEEE Signal Process. Lett.*, 18: 287-290. DOI: 10.1109/LSP.2011.2122333

Gonzalez, R.C. and R.E. Woods, 2006. *Digital Image Processing*. 2nd Edn., Prentice-Hall, Inc., Upper Saddle River, NJ, USA.

Gordon, W.J. and J.A. Wixom, 1978. Shepard's method of "Metric Interpolation" to bivariate and multivariate interpolation. *Math. Comput.*, 32: 253-264. DOI: 10.1090/S0025-5718-1978-0458027-6

Ko, S.J. and Y.H. Lee, 1991. Center weighted median filters and their applications to image enhancement. *IEEE Trans. Circuits Syst.*, 38: 984-993. DOI: 10.1109/31.83870

Nikolova, M., R.H. Chan and J.F. Cai, 2008. Two-phase approach for deblurring images corrupted by impulse plus gaussian noise. *Inverse Prob. Imag.*, 2: 187-204. DOI: 10.3934/ipi.2008.2.187

Pmathrmacuteal, L., R. Olmathrmacuteah-Gmathrmacuteal and Z. Makmathrmacuteo, 2009. Shepard interpolation with stationary points. *Acta Univ. Sapientiae. Inform.*, 1: 5-13.

Shepard, D., 1968. A two-dimensional interpolation function for irregularly-spaced data. *Proceedings of the 23rd ACM National Conference*, Aug. 27-29, ACM, USA, pp: 517-524. DOI: 10.1145/800186.810616

Srinivasan, K.S. and D. Ebenezer, 2007. A new fast and efficient decision-based algorithm for removal of high-density impulse noises. *IEEE Signal Process. Lett.*, 14: 189-192. DOI: 10.1109/LSP.2006.884018

Toh, K.K.V. and N.A.M. Isa, 2010. Noise adaptive fuzzy switching median filter for salt-and-pepper noise reduction. *IEEE Signal Process. Lett.*, 17: 281-284. DOI: 10.1109/LSP.2009.2038769

Toygar, Ö., H. Demirel and C. Kalyoncu, 2013. Interpolation-based impulse noise removal. *IET Image Process.*, 7: 777-785. DOI: 10.1049/iet-ipr.2013.0146

- Vijaykumar, V.R., G. Santhana Mari and D. Ebenezer, 2014. Fast switching based median-mean filter for high density salt and pepper noise removal. *AEU - Int. J. Electr. Commun.*, 68: 1145-1155.  
DOI: 10.1016/j.aeue.2014.06.002
- Wang, Z., A.C. Bovik, H.R. Sheikh and E.P. Simoncelli, 2004. Image quality assessment: From error visibility to structural similarity. *IEEE Trans. Image Process.*, 13: 600-612.  
DOI: 10.1109/TIP.2003.819861
- Wang, Z. and D. Zhang, 1999. Progressive switching median filter for the removal of impulse noise from highly corrupted images. *IEEE Trans. Circuits Syst.*, 46: 78-80. DOI: 10.1109/82.749102